Dynamical Suppression of $1/f$ Noise Processes in Qubit Systems

Lara Faoro[1,*] and Lorenza Viola[2,†]

[1]*Institute for Scientific Interchange Foundation, Viale Settimio Severo 65, I0133 Torino, Italy*
[2]*Los Alamos National Laboratory, Mail Stop B256, Los Alamos, New Mexico 87545, USA*

(Received 18 September 2003; published 18 March 2004)

We investigate the capability of dynamical decoupling techniques to reduce decoherence from a realistic environment generating $1/f$ noise. The predominance of low frequency modes in the noise profile allows for decoherence scenarios where relatively slow control rates suffice for a drastic improvement. However, the actual figure of merit is very sensitive to the details of the dynamics, with decoupling performance which may deteriorate for non-Gaussian noise and/or high frequency working points. Our results are promising for robust solid-state qubits and beyond.

DOI: 10.1103/PhysRevLett.92.117905 PACS numbers: 03.67.Pp, 03.65.Yz, 05.40.Ca, 89.75.Da

Noise processes characterized by a $1/f$ power spectrum are ubiquitously encountered in nature. While a unified theory of the underlying mechanisms remains elusive, $1/f$ noise plays a prominent role in dynamical phenomena as diverse as transport in electronic devices [1], light emission from astrophysical sources [2], statistics of DNA sequences [3], and stock market prices [4]. In recent years, the continuous advances witnessed by device nanotechnologies, along with the challenge to implement quantum information processing (QIP) in solid-state systems [5], have sharpened the demand for a detailed understanding of $1/f$ noise effects and for viable compensation schemes at the quantum level. In particular, $1/f$ noise due to fluctuating background charges (BCs) severely hampers the performance of single-electron tunneling devices [6] and Josephson qubits in the charge regime [7].

Prompted by the experimental demonstration of a coherent charge echo in a Cooper-pair box [8], efforts are underway to explore the possibility of $1/f$ noise reduction via active control techniques. Recent theoretical analyses [9,10] largely rely on deriving $1/f$ noise from the influence of an harmonic oscillator bath, e.g., through spin-boson models with sub-Ohmic damping [11]. While this accurately represents environments consisting of a *continuum* of weakly coupled modes, the inherent Gaussian distribution of the fluctuations fails at reproducing the distinctive properties of $1/f$ noise due to realistic *discrete* environments [12]. Compensation of non-Gaussian random telegraph noise (RTN) from a *single* bistable source is considered in [13]. However, an appropriate distribution of characteristic time scales is required to obtain genuine $1/f$ noise effects [14], thus qualitatively changing the nature of the control problem.

In this Letter, we present a comprehensive study of the effectiveness of decoupling methods [15,16] at suppressing $1/f$ noise in a single qubit. Our approach fully captures both Gaussian and non-Gaussian effects for realistic noise spectra and arbitrary operating points of the qubit. We find that the control performance depends critically on the frequency location of the dominating $1/f$ noise sources, the quality of the attainable suppression becoming comparatively higher as the latter shifts toward lower frequencies. For purely Gaussian $1/f$ dephasing, this implies the potential of significant coherence recovery (up to 75%) by using control rates which can be orders of magnitude slower than expected from the fastest characteristic time scale present in the system.

Noise model.—A simple way for generating a $1/f$ spectrum is via an ensemble of M independent, randomly activated bistable processes. Let $\xi_k(t)$ be an asymmetric RTN signal switching between values $\pm\nu_k/2$ with rates $\gamma_k^{(\pm)}$, $\gamma_k = \gamma_k^{(+)} + \gamma_k^{(-)}$. If a distribution $P(\gamma) \propto 1/\gamma$ is assumed for the switching rates $\gamma_k \in [\gamma_{\min}, \gamma_{\max}]$ [1,14], the total fluctuation $\Xi(t) = \sum_k \xi_k(t)$ exhibits a $1/f$ power spectrum of the form $S(|\omega|) = A/|\omega|$, $A > 0$, in a frequency range defined by effective cutoffs $\gamma^e_{\min} \gg \gamma_{\min}$, $\gamma^e_{\max} \ll \gamma_{\max}$. We focus on distributions of strengths ν_k sufficiently peaked around their mean value $\langle\nu\rangle \geq 0$, in which case A is proportional to the number n_d of fluctuators per noise decade, weighted by $\langle\nu\rangle^2$.

The above phenomenological model applies to a variety of $1/f$ noise processes, e.g., due to delocalized charge traps or hopping defects in solid-state devices [14]. In a fully quantum description, the RTN ensemble is replaced by an environment E consisting of M two-state BCs [17], each coupled with strength ν_k to the system and with strength T_k to an electronic band inducing relaxation with rate γ_k. Thus, $H_E = \sum_k H_k$, with

$$H_k = \epsilon_k b_k^\dagger b_k + T_k \sum_l [c_{kl}^\dagger b_k + \text{H.c.}] + \sum_l \varepsilon_{kl} c_{kl}^\dagger c_{kl}, \quad (1)$$

where ϵ_k, ε_{kl} are energy parameters and $b_k(b_k^\dagger)$, $c_{kl}(c_{kl}^\dagger)$ canonical fermion operators, respectively. The semiclassical approximation is accurate in a regime where $T_k \gg \nu_k$, implying the possibility to neglect quantum back-action effects from the system. Let $g_k = \nu_k/\gamma_k$ for each noise source. The resulting decoherence contribution is qualitatively different depending on whether $g_k \ll 1$ (Gaussian source) or not [12]. While purely Gaussian

noise may be formally reproduced by an appropriate bosonic bath [11], non-Gaussian $1/f$ behavior may exhibit nonequilibrium saturation features and pronounced non-Lorentzian line shapes [12].

Decoupling setting.—Our target system S is a single qubit, described by a Hamiltonian $H_S = -[\Omega\sigma_z + \Delta\sigma_x]/2$, σ_z eigenstates $\{|0\rangle, |1\rangle\}$ defining the computational basis, and $\Delta E = \sqrt{\Omega^2 + \Delta^2}$ giving the energy scale of the free dynamics ($\hbar = 1$). For the charge qubit realized in [7,8], Ω is the separation between the two lowest charge states, while Δ is the Josephson energy of the junction. Coupling with the BCs is introduced via a system-environment interaction $H_{\rm SE} = \sum_k v_k b_k^\dagger b_k \otimes \sigma_z$, corresponding semiclassically to $H_{\rm RTN}(t) = \Xi(t)\,\sigma_z$. Both relaxation and dephasing occur, depending on the longitudinal or transverse nature of the fluctuations relative to the physical basis defined by the energy eigenstates. When $\Delta = 0$, the physical and computational bases are aligned, and decoherence is purely adiabatic. In the opposite case where $\Omega = 0$, purely nonadiabatic dissipation and dephasing take place, both mechanisms influencing decoherence in the z basis as the latter is 90° displaced. Borrowing from the Cooper-pair-box terminology, we shall refer to these limiting situations as pure dephasing and charge degeneracy regimes, respectively [12].

Dynamical decoupling strategies coherently average out the effects of unwanted interactions over a sufficiently long time scale by means of a tailored control field [16]. In the simplest formulation, decoupling is achieved by subjecting the system to cyclic sequences of instantaneous (bang-bang) control pulses. We consider two elementary decoupling protocols specified by the following control cycles: $\mathcal{P}_A = \{\Delta t, \pi_x, \Delta t, \pi_{-x}\}$ (asymmetric) and $\mathcal{P}_S = \{\Delta t/2, \pi_x, \Delta t, \pi_{-x}, \Delta t/2\}$ (symmetric), where Δt and $\pi_{\pm x}$ denote a free evolution interval of duration Δt and a controlled rotation of 90° about the $\pm x$ axis, respectively. While the two implementations are equivalent in the ideal limit of arbitrarily fast control $\Delta t \to 0$, superior averaging is expected from the time-symmetric protocol in the realistic case of finite Δt, thanks to the cancellation of higher-order corrections [15,16,18].

Decoupled dynamics.—Complete information about the dissipative qubit dynamics is contained in the expectation values of the qubit observables σ_ℓ, $\ell = x, y, z$, after evolution in the presence of the $1/f$ disturbance with and without the decoupling field. For a generic H_S, the latter have been calculated numerically as the ensemble average over the stochastic qubit state evolved under $H_{\rm RTN}(t)$ [19], $\langle\sigma_\ell(t)\rangle = \mathcal{E}\{\langle\psi(t)|\sigma_\ell|\psi(t)\rangle\}$, starting from known pure-state initial conditions $|\psi(0)\rangle = c_0|0\rangle + c_1|1\rangle$, $|c_0|^2 + |c_1|^2 = 1$. We consider here two performance indicators: $\langle\sigma_+(t)\rangle = \langle\sigma_x(t) + i\sigma_y(t)\rangle/2$, starting from $c_0 = c_1 = 1/\sqrt{2}$, which describes coherence in the z basis; and $\langle\sigma_z(t)\rangle$, starting from $c_0 = 1$, $c_1 = 0$, which is a signature for coherent oscillations in the x basis. At $\Delta = 0$, an analytic benchmark has been obtained by both performing the semiclassical approximation in the Heisenberg equations of motion derived from Eq. (1) and by exactly solving the RTN dynamics. If $Z(t) = |\langle\sigma_+(t)\rangle/\langle\sigma_+(0)\rangle|$ defines the controlled decay function, the following expression holds in the presence of a single BC after a time $t = 2N\Delta t$ corresponding to N control cycles [19]:

$$Z(t) = a^N\left\{\frac{f(\alpha) + f(-\alpha)}{4}\,{}_2F_1\left[\frac{1-N}{2}, 1 - \frac{N}{2}; 1 - N; z^2\right] - |\alpha|^4\,{}_2F_1\left[1 - \frac{N}{2}, \frac{3}{2} - \frac{N}{2}; 2 - N; z^2\right]\right\}. \quad (2)$$

Here, ${}_2F_1$ denotes the regularized hypergeometric function [20], $\alpha = \sqrt{1 - g^2 - 2ig\tanh(\epsilon/2k_BT)} = \alpha' + i\alpha''$, $z = 2e^{-\gamma\Delta t}/a$, and a, $f(\alpha)$ are, respectively, given by

$$a = \frac{e^{-\gamma\Delta t}}{|\alpha|^2}[(1 + g^2 + |\alpha|^2)\cosh(\gamma\alpha'\Delta t) - (1 + g^2 - |\alpha|^2)\cos(\gamma\alpha''\Delta t)],$$

$$f(\alpha) = e^{\alpha'\Delta t}\{|\alpha|^2 + [1 + g^2 - 2ig(\delta p_{\rm eq} - \delta p_0)] + 2(\alpha' + \delta p_0 g\alpha'')\} + e^{i\alpha''\Delta t}\{2i(\alpha'' + \delta p_0 g\alpha') + |\alpha|^2 - [1 + g^2 - 2ig(\delta p_{\rm eq} - \delta p_0)]\},$$

$\delta p_{\rm eq} = \tanh(\epsilon/2k_BT)$ and $\delta p_0 = \pm 1$ denoting the equilibrium and initial value of the BC population difference.

For M noise sources, the individual contributions factorize, $Z(t) = \prod_k Z_k(t)$. In the absence of control, the result of [12], Eq. (4), is recovered. In the continuous limit where $\Delta t = t/N \to 0$ [16], one can prove using Eq. (2) that $Z_k(t) \to 1\ \forall\, k$, confirming perfect decoherence suppression for ideal decoupling. Thus, *complete* $1/f$ compensation requires access to control time scales $\Delta t \lesssim 1/\gamma_{\rm max}$, so as to quench the influence of the *fastest* fluctuator present in the environment. We find that an almost full coherence recovery (better than 90%) can always be achieved if decoupling is fast relative to the *effective upper cutoff*, $\Delta t \lesssim 1/\gamma^e_{\rm max}$, implying controls up to an order of magnitude slower. Tighter estimates of the minimum control rates able to ensure a significant decoherence suppression are possible upon identifying the dominant noise sources in the relevant dynamical regime. While a detailed analysis is deferred to [19], the salient features may be summarized as follows.

Decoupling in the pure dephasing regime.—Adiabatic decoherence is insensitive to the energy scale $\Delta E = \Omega$, but critically dependent on the coupling strength distribution, the overall time scale of the process being largely determined by $\langle v\rangle$ for small dispersions as assumed. An important consequence of ΔE being irrelevant is that *decoherence acceleration* [16] is *never* observed for $\Delta = 0$ with arbitrary control parameters. Symmetric decoupling performs systematically better over its

asymmetric counterpart, differences being larger for a number of control cycles $N \lesssim 5$. For charge-echo sequences with realistic non-Gaussian noise and Δt values [8], the symmetric readout signal can be up to 70% higher at times where the free coherence has entirely decayed (Fig. 1). Effects related to temperature as well as different initializations of the BCs (including sample to sample variations and correlations when repetitions of the readout process are needed as in [8]) can be fully taken into account [19]. While this may be critical for a quantitative comparison with experiments, we anticipate no substantial changes as far as the decoupling efficacy is concerned.

A key factor determining the control effectiveness for dephasing processes is *where* $\langle \nu \rangle$ is positioned within $[\gamma_{\min}, \gamma_{\max}]$. For purely Gaussian noise, $\nu_k/\gamma_k \ll 1 \ \forall \ k$, thus $\langle \nu \rangle \lesssim \gamma_{\min}$ for realistic spectra. Gaussian dephasing is dominated by the lowest spectral components, as witnessed by the diverging rate predicted by second-order perturbation theory for $\omega \to 0$. Hence, averaging of the slowest decades near $\gamma_{\min}$ suffices for a dramatic coherence improvement [Fig. 2(a)]. Non-Gaussian behavior may arise either for a lower $\gamma_{\min}$ at fixed $\langle \nu \rangle$ [Fig. 2(b)], or for a higher $\langle \nu \rangle$ in a fixed range $[\gamma_{\min}, \gamma_{\max}]$ [Fig. 2(c)]. Irrespective of whether saturation effects occur for non-Gaussian charges [12,19], a substantial decoherence contribution originates from noise decades near $\langle \nu \rangle$, thus making their compensation essential. In practice, an operational criterion to obtain between 60%–75% coherence recovery is to choose $\Delta t \lesssim \min(1/10^q \gamma_{\min}, 1/10^q \langle \nu \rangle)$, with $q = 1$ or 2 at most. For fixed $\gamma_{\min}$, this allows for pulse repetition times which can be longer and longer the lower the value of $\langle \nu \rangle$. In a strongly non-Gaussian regime where the latter moves to higher frequencies, the advantages of slow decoupling are lost, and control rates ruled by $\gamma^e_{\max}$, $\gamma_{\max}$ become necessary.

Decoupling in the charge degeneracy regime.—A distinctive feature of the dissipative dynamics in this limit is the sensitivity to the energy scale $\Delta E = \Delta$. For Gaussian noise, this may be understood from the fact that both relaxation and dephasing are governed (up to a factor 2) by a single rate, which depends only on the power spectrum $S(\omega = \Delta E)$ to second order in the couplings. We find that the dynamical role of the energy scale ΔE extends beyond the Gaussian limit. In particular, irrespective of the Gaussian or non-Gaussian nature of the spectrum, decoherence rates at charge degeneracy do not substantially differ from adiabatic ones if the qubit operates at sufficiently low frequencies, $\Delta E \to \gamma_{\min}$. Shifting the working point to higher frequency has the effect of filtering out the majority of noise contributions, leading to coherence times which are orders of magnitude longer than in the corresponding dephasing configuration

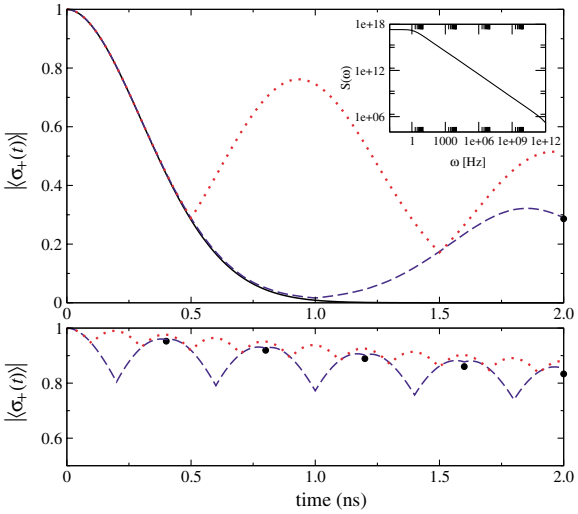

FIG. 1 (color online). Symmetric ($\mathcal{P}_S$, dotted) vs asymmetric ($\mathcal{P}_A$, dashed) decoupling for pure dephasing from a realistic $1/f$ spectrum [8] [Inset: $\gamma_{\min} = 1$ Hz (extrapolated), $\gamma_{\max} = 10^{12}$ Hz, $n_d = 1000$, $\langle \nu \rangle = 9.2 \times 10^7$ Hz, $\Delta\nu/\langle \nu \rangle \sim 0.2$]. Upper panel: free evolution (solid line) vs echo signals, $\Delta t = 1$ ns. Lower panel: $N = 5$, $\Delta t = 0.2$ ns. Stroboscopic data points from Eq. (2) are shown at $t = 2N\Delta t$, whereas continuous curves result from averaging over 10^5 RTN realizations. Each BC is initially assumed in a thermal mixture with $\epsilon/2k_BT \simeq \delta p_{\rm eq} = 0.08$.

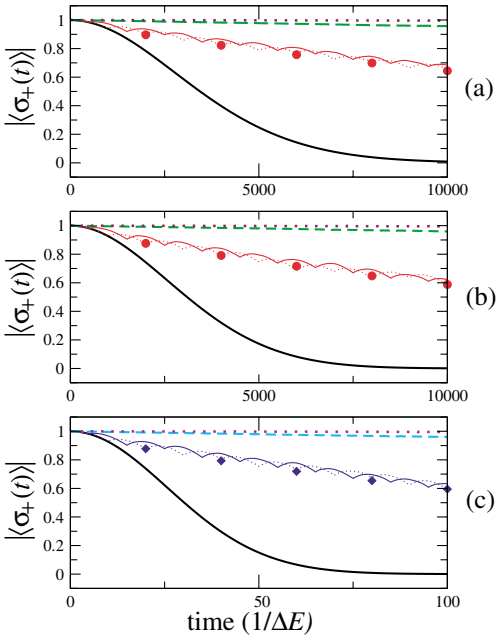

FIG. 2 (color online). $1/f$ suppression under pure dephasing conditions, $\Omega = 1$, $\Delta = 0$. Top to bottom: (a) Purely Gaussian spectrum, $\gamma_{\min} = 10^{-4}$, $\gamma_{\max} = 100$, $n_d = 100$, $\langle \nu \rangle = 10^{-4}$; (b), (c) Non-Gaussian spectra with parameters as in (a) except that $\gamma_{\min} = 10^{-6}$ in (b), and $\langle \nu \rangle = 0.01$ in (c), respectively. $\gamma^e_{\max} = 10$ in all cases. Solid lines depict free evolutions. Control parameters are (a) and (b) $\Delta t = 1000$ (thin solid line), $\Delta t = 100$ (dashed line), $\Delta t = 10$ (dotted line); (c) $\Delta t = 10$ (thin solid line), $\Delta t = 1$ (dashed line), $\Delta t = 0.1 \sim 1/\gamma^e_{\max}$ (dotted line). Results are averages over 2×10^4 RTN realizations under $\mathcal{P}_S$ protocols. Each BC is initially in a pure state randomly sampled according to $\langle \delta p_0 \rangle = \delta p_{eq} = 0.08$. Asymmetric RTN and analytic results from Eq. (2) are also shown for $N = 5$ cycles.

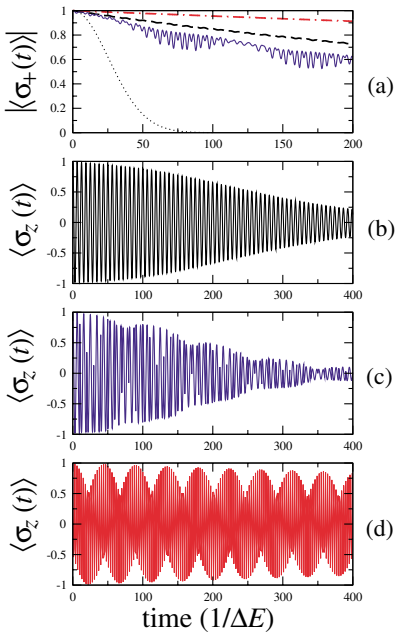

FIG. 3 (color online). $1/f$ suppression under charge degeneracy conditions, $\Omega = 0$, $\Delta = 1$. Noise spectrum as in Fig. 2(c). (a) Coherence in the z basis for free (dashed line) and controlled dynamics, $\Delta t = 10$ (solid line), $\Delta t = 1$ (dash-dotted line). The dephasing curve at $\Delta E = 1$ is reproduced from Fig. 2(c) (dotted line). Note the deteriorated performance for $\Delta t = 10$. Lower panels: damping [(b), no control], acceleration [(c), $\Delta t = 10$], and partial recovery [(d), $\Delta t = 1$] of coherent charge oscillations. Complete recovery (not shown) is found for $\Delta t = 0.1 \sim 1/\gamma^e_{\max}$. RTN averages ($\mathcal{P}_S$ protocols) are taken over 2×10^5 realizations, with environment initialized as in Fig. 2.

[Fig. 3(a)]. However, a hallmark of control in this regime is the possibility to *accelerate* decoherence if cycle times long with respect to the free period $2\pi/\Delta E$ are used. This is evident in the oscillatory dynamics of $\langle \sigma_z(t) \rangle$ [Figs. 3(b)–3(d)]. If $\Delta t \gg \pi/\Delta E$, the improvement in the controlled amplitude does not compensate for the effective decay due to the frequency mismatch relative to the free oscillations, and overall acceleration results [19]. As Δt approaches $\pi/\Delta E$ from above, the relative importance of these two mechanisms reverses, and a crossover to noise suppression occurs at times which are shorter for shorter Δt. Full coherence recovery is guaranteed for $\Delta t \lesssim 1/10\Delta E$ which, however, may be close to $1/\gamma^e_{\max}$ if ΔE is large.

Interestingly, a trade-off emerges in the charge degeneracy regime between noise effects which are stronger but easier to decouple (as ΔE shifts toward low frequencies); and noise effects which are substantially reduced from the beginning but harder to suppress (as ΔE increases). A similar conclusion is likely to hold for generic qubit parameters. Thus, while it may seem counterproductive to consider low operation frequencies in the presence of $1/f$ noise, in practice both the relevant noise level and the available control resources should guide the choice of a working point able to maximize the control efficiency.

We have characterized the performance of decoupling techniques at reducing $1/f$ noise based on a realistic model. Beside identifying noise scenarios where decoupling is highly effective with affordable rates, our results suggest the possibility of using control as a *diagnostic tool* to infer spectral properties (such as $\langle v \rangle$ or $\gamma^e_{\max}$), which are not directly measurable. While actual details will be device dependent and require a dedicated analysis incorporating the underlying physics, we expect that our main conclusions will have a wide range of applicability, including noise spectra with power-law behavior of the form $1/f$ with $\alpha > 1$ [1], or alternative qubit design as demonstrated in [21]. Ultimately, our results hold the promise that decoupling methods may substantially improve the prospects for reliable solid-state QIP.

L. F. acknowledges support from Los Alamos National Laboratory, where this work was initiated, and from the EU(IST-FET-SQUBIT). It is a pleasure to thank P. Giorda, E. Knill, and R. Onofrio for discussions.

*Electronic address: faoro@isiosf.isi.it
†Electronic address: lviola@lanl.gov

[1] M. B. Weissman, Rev. Mod. Phys. **60**, 537 (1988).
[2] W. H. Press, Comments Astrophys. **7**, 103 (1978).
[3] R. F. Voss, Phys. Rev. Lett. **68**, 3805 (1992).
[4] A. W. Lo, Econometrica **59**, 1279 (1991).
[5] Special focus issue on *Experimental Proposals for Quantum Computation* [Fortschr. Phys. **48** (2000)].
[6] M. Covington, M. W. Keller, R. L. Kautza, and J. Martinis, Phys. Rev. Lett. **84**, 5192 (2000).
[7] Y. Nakamura, Y. A. Pashkin, and J. S. Tsai, Nature (London) **398**, 786 (1999).
[8] Y. Nakamura, Y. A. Pashkin, T. Yamamoto, and J. S. Tsai, Phys. Rev. Lett. **88**, 047901 (2002).
[9] J. M. Martinis *et al.*, Phys. Rev. B **67**, 094510 (2003).
[10] K. Shiokawa and D. A. Lidar, Phys. Rev. A **69**, 030302 (2004).
[11] A. Shnirman, Y. Makhlin, and G. Schön, Phys. Scr. **T102**, 147 (2002).
[12] E. Paladino, L. Faoro, G. Falci, and R. Fazio, Phys. Rev. Lett. **88**, 228304 (2002).
[13] H. Gutmann, F. K. Wilhelm, W. M. Kaminsky, and S. Lloyd, quant-ph/0308107.
[14] P. Dutta and P. M. Horn, Rev. Mod. Phys. **53**, 497 (1981).
[15] U. Haeberlen, *High Resolution NMR in Solids: Selective Averaging* (Academic, New York, 1976).
[16] L. Viola and S. Lloyd, Phys. Rev. A **58**, 2733 (1998); L. Viola, E. Knill, and S. Lloyd, Phys. Rev. Lett. **82**, 2417 (1999); L. Viola and E. Knill, Phys. Rev. Lett. **90**, 037901 (2003).
[17] R. Bauernschmitt and Y. V. Nazarov, Phys. Rev. B **47**, 9997 (1993).
[18] S. Gheorghiu-Svirschevski, Phys. Rev. A **66**, 032101 (2002).
[19] L. Faoro and L. Viola (to be published).
[20] M. Abramowitz and I. A. Stegun, *Handbook of Mathematical Functions* (Dover, New York, 1970), p. 556.
[21] D. Vion *et al.*, Science **296**, 886 (2002).